

# 100th Anniversary of Macromolecular Science Viewpoint: Single-Molecule Studies of Synthetic Polymers

Danielle J. Mai\* and Charles M. Schroeder\*

Cite This: *ACS Macro Lett.* 2020, 9, 1332–1341

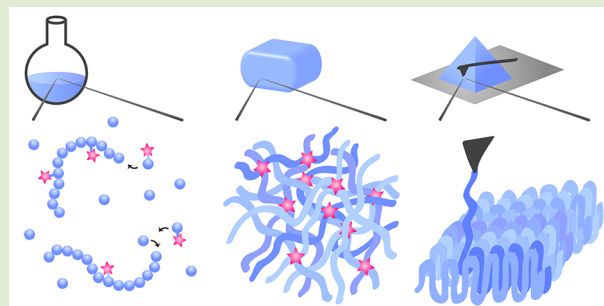
Read Online

ACCESS |

Metrics &amp; More

Article Recommendations

**ABSTRACT:** Single polymer studies have revealed unexpected and heterogeneous dynamics among identical or seemingly similar macromolecules. In recent years, direct observation of single polymers has uncovered broad distributions in molecular behavior that play a key role in determining bulk properties. Early single polymer experiments focused primarily on biological macromolecules such as DNA, but recent advances in synthesis, imaging, and force spectroscopy have enabled broad exploration of chemically diverse polymer systems. In this Viewpoint, we discuss the recent study of synthetic polymers using single-molecule methods. In terms of polymer synthesis, direct observation of single chain polymerization has revealed heterogeneity in monomer insertion events at catalytic centers and decoupling of local and global growth kinetics. In terms



of single polymer visualization, recent advances in super-resolution imaging, atomic force microscopy (AFM), and liquid-cell transmission electron microscopy (LC-TEM) can resolve structure and dynamics in single synthetic chains. Moreover, single synthetic polymers can be probed in the context of bulk material environments, including hydrogels, nanostructured polymers, and crystalline polymers. In each area, we highlight key challenges and exciting opportunities in using single polymer techniques to enhance our understanding of polymer science. Overall, the expanding versatility of single polymer methods will enable the molecular-scale design and fundamental understanding of a broad range of chemically diverse and functional polymeric materials.

When Staudinger controversially proposed<sup>1</sup> and subsequently proved<sup>2</sup> the chemical structure of macromolecules, the notion of directly observing a single polymer chain was unimaginable. Experimental advances have since enabled the isolation and interrogation of individual polymer molecules: fluorescence microscopy provided the first visualization of single polymer dynamics,<sup>3</sup> magnetic tweezers were used to measure the elasticity of single polymer chains,<sup>4</sup> and optical trapping was used to directly show tube-like or “reptative” polymer motion in an entangled polymer solution.<sup>5</sup> In parallel, atomic force microscopy (AFM) enabled direct observation of polymer chain packing<sup>6</sup> and expanded the range of single-molecule force measurements into the high-force regime (>100 pN).<sup>7,8</sup> The ability to observe polymer chain conformations revealed heterogeneous dynamics in an ensemble of seemingly identical polymers,<sup>9,10</sup> coined “molecular individualism,” in addition to revealing other dynamic phenomena including conformational hysteresis in strong flows<sup>11</sup> to hindered stretching of architecturally complex polymers in flow.<sup>12–14</sup> A common thread between these discoveries is the importance and role of molecular distributions to all aspects of polymer science and engineering.

Early single polymer experiments focused on biological macromolecules, particularly using double-stranded deoxyribo-

nucleic acid (DNA) for polymer dynamics or mechanical studies.<sup>3–5</sup> DNA serves as an accessible model system due to the routine preparation of monodisperse, high-molecular weight samples, including commercially available bacteriophage DNA (T7, Lambda, and T4; unstained contour lengths ranging from 13–56  $\mu\text{m}$ ). Practical considerations for single-molecule experiments using DNA include the ability to fluorescently label the double-helix backbone for real-time observation of the polymer contour,<sup>3,5</sup> as well as the incorporation of distinct chemical or bioorthogonal moieties at the 5' and 3' ends of DNA to tether molecules to surfaces and microparticles for further manipulation.<sup>4,5</sup> Robust and established protocols for DNA labeling, tethering, and manipulation have enabled a broad array of single polymer investigations by polymer physicists, chemists, and engineers.

Received: July 17, 2020

Accepted: August 25, 2020

Published: August 28, 2020



The fundamental understanding gained from single polymer experiments on biological macromolecules has recently been leveraged to enable single-molecule studies of synthetic organic polymers.<sup>15,16</sup> On the one hand, DNA and synthetic polymers exhibit universal scaling behavior of physical properties,<sup>17,18</sup> for example, universality in the swelling of the viscosity radius and the hydrodynamic radius.<sup>19</sup> On the other hand, local chemical interactions may lead to different behaviors for different polymer chemistries in complex environments such as melts, copolymer assemblies, and crystalline domains. Moreover, local properties such as backbone flexibility and monomer aspect ratio influence global properties such as chain elasticity and intramolecular hydrodynamic interactions (HI).<sup>18,20</sup> From this view, there are compelling reasons to extend the field of single polymer dynamics beyond DNA and to study the dynamics and properties of synthetic polymers at the molecular level. Some of the first single-molecule studies of synthetic polymers adapted single-molecule force spectroscopy (SMFS) to investigate the stretching mechanics of polystyrene chains.<sup>15,16</sup> These studies demonstrated smooth force–extension behavior of synthetic polymers, in contrast to “over-stretching” transitions observed in DNA and dextrans that undergo intramolecular conformational changes.<sup>7,21</sup> The molecular properties of numerous synthetic polymers were then determined by analyzing SMFS experiments with single-chain elasticity models and are extensively reviewed elsewhere.<sup>22,23</sup>

In this Viewpoint, we highlight recent single-molecule investigations of synthetic organic polymers (Figure 1). Our

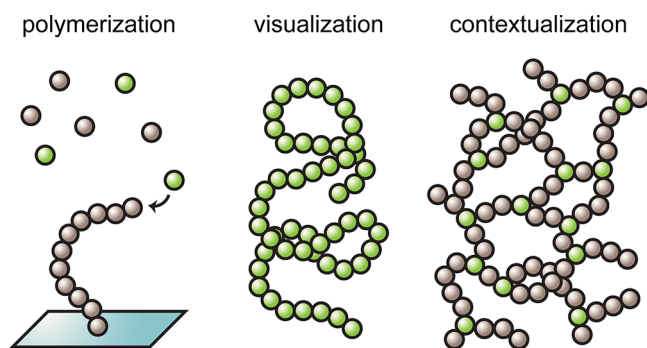


**Figure 1.** Single-molecule investigations of synthetic polymers explore monomer insertion kinetics, polymer chain conformations, and network structure heterogeneity.

discussion begins with single-molecule studies of polymer synthesis, where polymer chain growth is tracked using new catalysts and monomers. We then discuss the direct visualization of single polymer chains using recent advances in super-resolution optical microscopy, atomic force microscopy, and label-free electron microscopy. Finally, we explore single polymers probed in context, including cross-link junctions mapped in hydrogel networks, block copolymers assembled into nanostructures, and single polymers extracted from crystalline materials. In all cases, we identify key challenges and new opportunities for single-molecule experiments to provide further insight into polymer behavior.

## ■ SINGLE POLYMER SYNTHESIS AND KINETICS

Several polymerization methods rely on statistical processes that lead to dispersity and heterogeneity within a polymer sample. Polydispersity and sequence heterogeneities impact physico-chemical properties and behavior related to polymer processing,

self-assembly, and crystallization. From this view, understanding how distributions in molecular weight and sequence heterogeneity emerge can improve synthetic control, physical property prediction, and polymer informatics.<sup>24</sup> Sample distributions are traditionally monitored using analytical techniques with inherent ensemble averaging, and ensemble-averaged measurements mask the behavior of individual catalysts and polymer chains throughout a reaction. Early efforts toward unraveling polymerization kinetics at the single-molecule level tracked the diffusion of fluorescent dyes in the polymerization environment,<sup>25–29</sup> but these studies generally lacked quantitative information regarding the growth of nascent polymer chains. In recent years, single-chain experiments have shed new light on polymerization processes and kinetics.

Early single-chain studies analyzed surface-initiated polymerization by “freezing” ensembles of growing polymers to directly measure chain contour lengths using AFM-based SMFS.<sup>30</sup> Specifically, Lee-Thedieck and co-workers grafted poly-(hydroxyethyl methacrylate) (HEMA) from glass surfaces via surface-initiated reversible addition–fragmentation chain transfer (SI-RAFT). SI-RAFT reactions were quenched at predetermined intervals, after which RAFT chain ends underwent aminolysis to generate terminal thiol groups. Terminal thiols were then readily linked to gold-coated AFM cantilevers for SMFS of individual polymer chains (Figure 2A). Force–extension curves showed increasing chain contour lengths as a function of polymerization time, and these observations were supported by bulk measurements of surface thickness using tapping-mode AFM and ellipsometry.

During SI-RAFT reactions, solution-based RAFT reactions also proceed, thereby allowing for direct comparisons between solution- and surface-based polymerization of PHEMA.<sup>30</sup> Initially, the average molecular weight increased rapidly in both solution-based and SI-RAFT. At longer times, however, the average molecular weight reached a plateau in solution-based RAFT, in contrast to prolonged extension of chains grown on surfaces. The molecular weight distributions also diverged: SI-RAFT polymers were characterized by a narrow distribution with  $\bar{D} \approx 1.1$ , whereas polymers in solution reached  $\bar{D} \approx 1.8$  after 6 h.<sup>30</sup> The broader molecular weight distribution in solution was attributed to a fraction of low-molecular-weight chains that may have resulted from bimolecular termination events. This difference revealed a shortcoming of SMFS to characterize *ex situ* reactions, wherein chains that underwent early termination also lacked a terminal thiol group and were therefore excluded from SMFS analysis. Broadly speaking, this work represents a key step forward in understanding polymerization reactions at the molecular level as one of the first to apply SMFS to study polymer chain growth.

Using a clever adaptation of magnetic tweezers, researchers also studied single chain growth in ring-opening metathesis polymerization (ROMP) with SMFS.<sup>31</sup> Here, reactive polynorbornene chains were tethered between glass coverslips and magnetic particles coated with second-generation Grubbs’ ruthenium catalyst (G2; Figure 2B). Dual-tethered polynorbornene molecules were held at constant force to achieve a constant fractional chain extension, defined as the ratio between the chain extension and the polymer contour length, as described by the worm-like chain (WLC) model.<sup>32</sup> The magnetic tweezers’ *z*-position was stabilized for each molecule prior to initiating ROMP by the introduction of  $10^7$  excess norbornene relative to G2. During single polymer growth, the *z*-position was tracked

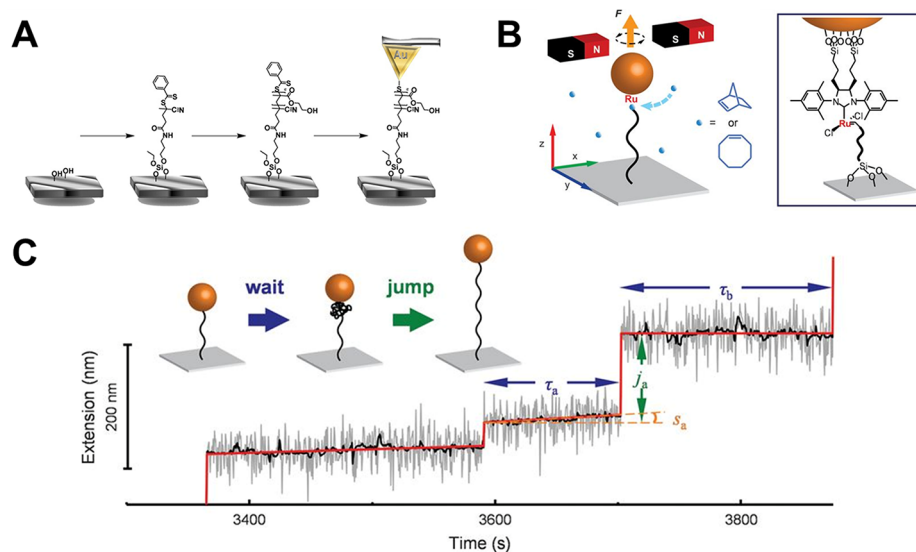


**Figure 2.** SMFS used to monitor single polymer growth via (A) atomic force microscopy and (B) magnetic tweezers. (C) Single-molecule extension of a growing polynorbornene chain exhibits “wait-and-jump” behavior. Waiting periods are characterized by wait time  $\tau$  and slope  $s$ , and jumps are characterized by jump length  $j$ . Inset: schematic of temporarily entangled polymer structure. (A) Adapted with permission from Tischer, T.; Gralla-Koser, R.; Trouillet, V.; Barner, L.; Barner-Kowollik, C.; Lee-Thedieck, C. *ACS Macro Letters* **2016**, *5* (4), 498–503. Copyright 2016 American Chemical Society. (B, C) Adapted and reprinted with permission from Liu, C.; Kubo, K.; Wang, E.; Han, K.-S.; Yang, F.; Chen, G.; Escobedo, F. A.; Coates, G. W.; Chen, P. *Science* **2017**, *358* (6361), 352–355. Copyright 2017 AAAS.

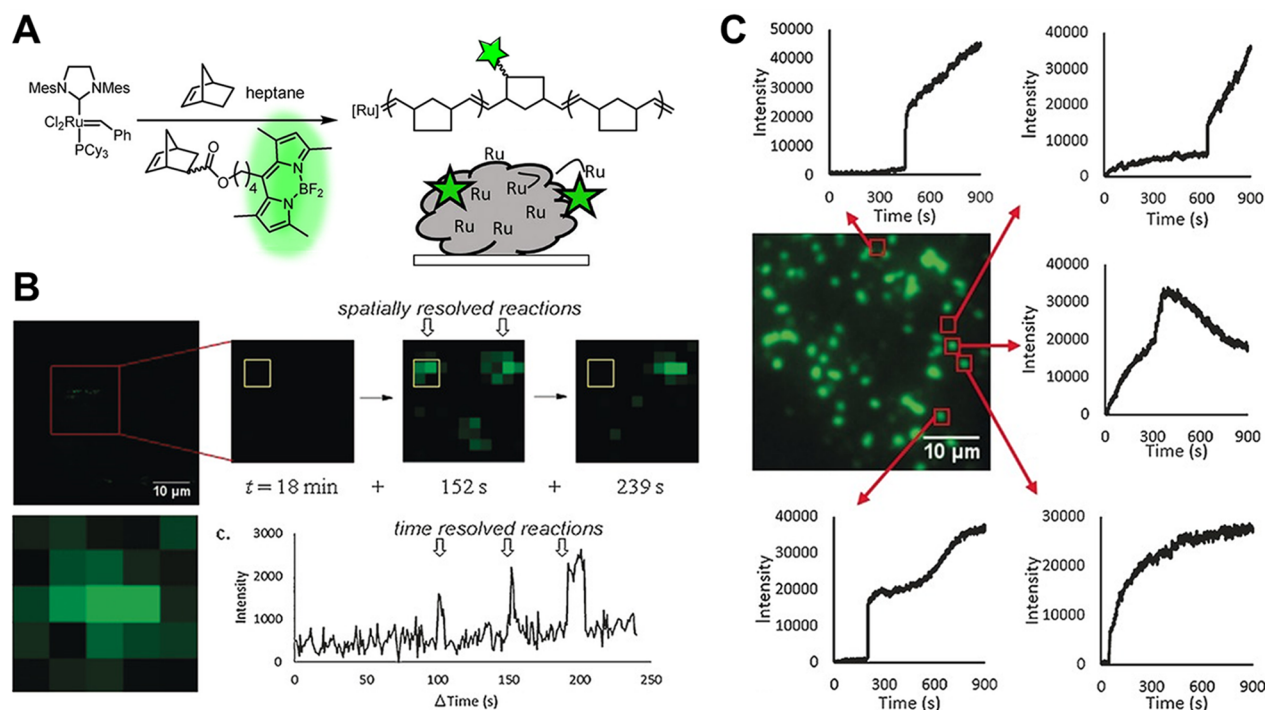


**Figure 3.** Single-molecule fluorescence microscopy reveals heterogeneous polymerization kinetics. (A) G2 catalysts are coprecipitated with polynorbornene to form surface aggregates. Adapted with permission from Easter, Q. T.; Blum, S. A. *Accounts of Chemical Research* **2019**, *S2* (8), 2244–2255. Copyright 2019 American Chemical Society. (B) Observation of single norbornene–BODIPY insertion events using TIRF mode. Monomer insertions are resolved in space and time. Adapted with permission from ref 33. Copyright 2017 Wiley-VCH Verlag GmbH & Co. KGaA. (C) Increasing the concentration of fluorescent norbornene–BODIPY enables kinetic measurements, which reveal heterogeneous polymerization rates between different surface aggregates. Intensity traces reflect  $0.29 \mu\text{m}^2$  regions (red boxes) within single aggregates of polynorbornene (green particles, image from  $t = 300 \text{ s}$ ). Adapted with permission from ref 35. Copyright 2018 Wiley-VCH Verlag GmbH & Co. KGaA.

with 6 to 10 nm precision, and monomer addition corresponded to increasing polymer extension under constant force.<sup>31</sup>

Single growing polymer chains revealed unexpected extension behavior, where “wait-and-jump” steps were observed instead of smooth, continuous growth (Figure 2C).<sup>31</sup> Waiting times  $\tau$

spanned hundreds of seconds and preceded nearly instantaneous jump lengths  $j$  up to  $\sim 10^3 \text{ nm}$  (thousands of monomers over 0.05 s), suggesting that chain growth occurred primarily during waiting periods. During the waiting periods, some extension trajectories exhibited slight increases over time,

reflected by the positive slope  $s$  in Figure 2C. Polymer conformations were visualized using molecular dynamics simulations, which suggested that monomer insertion introduces torsional strain to the polymer chain. Strained polymers are hypothesized to form temporarily entangled “hairball” conformations that eventually relax to produce spontaneous jumps in extension. The slope  $s$  of the waiting period describes the temporarily entangled structure, such that looser structures will expand during polymerization to produce larger slopes. Both the slope and the wait time were not significantly correlated with the jump length, suggesting that local catalyst configurations were unexpectedly decoupled from globally strained polymers. Overall, this landmark study revealed the need to understand and characterize monomer insertion events at the single chain level to understand polymer growth. The new insights revealed by these experiments could be used to guide the design of monomer species to tune insertion kinetics and subsequently control polymer growth.

Recently, Blum and co-workers pioneered an interesting set of studies of polymerization kinetics at the monomer scale by tracking G2 catalyst turnover events using single-molecule fluorescence microscopy.<sup>33–37</sup> This collective body of work revealed heterogeneous behavior of single catalysts by integrating approaches from organometallic molecular chemistry, fluorescent probe design, and quantitative imaging. Reactive polynorbornene chains and G2 catalysts were colocalized at coverslip surfaces by precipitation;<sup>33</sup> this strategy enabled specific detection of fluorescent probes near the surface using total internal reflectance fluorescence (TIRF) imaging without requiring tethers (Figure 3A). After precipitation, polymerization was initiated by addition of commercial norbornene and fluorescent norbornene–BODIPY conjugates. At low concentrations of fluorescent monomers ( $\sim 10^{-12}$  M),<sup>33,34</sup> monomer insertion events appeared as single flashes at polymer-rich regions on the coverslip. Rapid photobleaching of fluorescent tags allowed single chemical reactions to be spatially and temporally resolved (Figure 3B).

Sparse sampling from single-insertion events generally precluded quantitative analyses of chemical kinetics.<sup>34</sup> However, increasing the fluorescent monomer concentration revealed unexpected heterogeneous and dynamic chemical kinetics at catalytic centers.<sup>34,35</sup> Figure 3C illustrates transient traces of fluorescence intensity for different polynorbornene aggregates exposed to the same experimental conditions ( $\sim$ nM tagged norbornene and  $\sim$ mM untagged norbornene in heptane).<sup>35</sup> Initial step-like increases in fluorescence intensity correspond to polynorbornene precipitation at the surface. Precipitation is followed by heterogeneous behavior ranging from continuous linear growth (top), nonmonotonic changes in intensity suggesting slow polymerization relative to photobleaching (middle), and gradually changing polymerization rates (bottom). This study quantified a broad range of polymerization rates from  $10^4$  to  $10^6$  monomers per second.<sup>35</sup> Perhaps most importantly, this work provided key evidence supporting the notion that monomer insertion is a dynamic process as suggested by the decoupling of local and global configurations observed during SMFS of polynorbornene chain growth. Blum and co-workers further demonstrated the utility of single-molecule polymerization studies by exploring ROMP kinetics over 9 orders of magnitude in concentration.<sup>34</sup> Overall, this work revealed a powerful progression from single-monomer insertion reactions to subensemble kinetic states to fully averaged ensemble kinetics.

Broadly, these findings mark the beginning of exciting efforts to understand polymerization kinetics at the level of single chains and monomers. In addition, recent kinetic studies have explored supramolecular polymer assembly<sup>38</sup> and ring-expansion polymerization.<sup>39</sup> Future opportunities include gaining deeper insight into the role of heterogeneous reaction kinetics on local chain structure and properties (especially for copolymers), adapting single-molecule methods to study broader classes of polymerization reactions, and investigating single chain polymerization in solution. In this way, single molecule techniques will be used to answer key unresolved questions regarding the physicochemical limits of uniformity (or lack thereof) during polymerization reactions, thereby opening new avenues to control polymer synthesis. Potential methods to study solution-based polymerization include nanopore detection methods<sup>40</sup> and automated flow control methods for soft material dynamics and molecular rheology.<sup>41–43</sup>

## ■ DIRECT VISUALIZATION OF SINGLE POLYMER CHAINS

Direct observation of a polymer backbone or chain contour poses distinct challenges compared to using force-based methods to study polymerization kinetics. Moreover, real-time visualization of single synthetic polymers using fluorescence microscopy poses additional technical challenges compared to imaging single DNA polymers. Several bright and photostable fluorescent dyes for DNA are designed to intercalate along the DNA double helix backbone, which avoids the need for covalent dye attachment to the polymer backbone. In addition, several nucleic acid dyes (e.g., cyanine dimers) are intrinsically nonfluorescent in the unbound state, offering straightforward labeling methods without the need for purification of excess, unbound dye. This labeling strategy has enabled single-molecule visualization of natural DNA polymers and hybrid biosynthetic polymers composed of DNA with grafted poly(*N*-isopropylacrylamide) (pNIPAM).<sup>44</sup> Although synthetic pNIPAM branches were not explicitly visualized, these hybrid polymers exhibited thermoresponsive conformational dynamics due to temperature-dependent, hydrophilic-to-hydrophobic transitions of pNIPAM.

Fluorescence imaging of single synthetic polymers requires sufficient contrast, signal-to-noise, and signal-to-background intensities in aqueous or nonaqueous systems. In some cases, organic solvents contain aromatic groups that are naturally fluorescent, resulting in an undesirable increase in background fluorescence. In general, fluorescence imaging of naturally nonfluorescent synthetic polymers requires the introduction of fluorescent dyes or labels via covalent attachment, which can result in uneven distribution along the backbone, alteration of the physical properties of the polymer chains, and formation of larger aggregates.<sup>45</sup> Electron microscopy proves challenging because polymers composed of lighter elements exhibit weak electron-optical image contrast and are sensitive to radiative damage. Contrast generated with heavy element staining is limited to specific backbone chemistries and can introduce nanostructural artifacts.<sup>46,47</sup> Weak contrast is directly related to temporal resolution, for which needs vary dramatically depending on the property of interest and the broad spectrum of relevant time scales in polymeric systems.

Spatial resolution presents an additional challenge, wherein the Abbe diffraction limit prevents imaging of subwavelength structures. Conventional optical microscopy can resolve features down to  $\approx 250$  nm, which falls short of the nanometer-scale

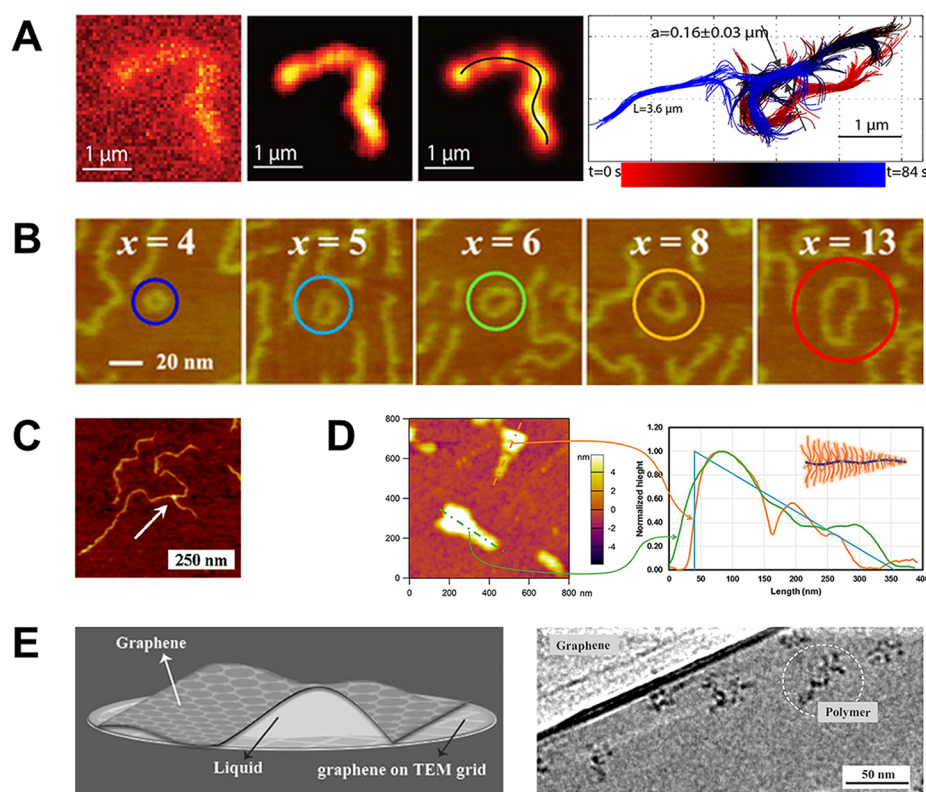


**Figure 4.** Comparison of high-resolution techniques to visualize single polymer chains. (A) Fluorescence images of poly(isocyanop-L-alanine propargylperylene diimide) in a matrix of unlabeled poly(isocyanop-L-alanyl-D-alanine methyl ester). Left to right: raw, background-subtracted, and reconstructed images of the chain contour. The plot superimposes reconstructed contours of a polymer undergoing reptation. Adapted with permission from Keshavarz, M.; Engelkamp, H.; Xu, J.; Braeken, E.; Otten, M. B. J.; Uji-i, H.; Schwartz, E.; Koepf, M.; Vananroye, A.; Vermant, J.; Nolte, R. J. M.; De Schryver, F.; Maan, J. C.; Hofkens, J.; Christianen, P. C. M.; Rowan, A. E. *ACS Nano* **2016**, *10* (1), 1434–1441. Copyright 2016 American Chemical Society. (B) AFM height images display cyclic polymer brushes synthesized using multimeric ring expansion. AFM resolves rings with different numbers of multimers  $x$ . Reprinted with permission from Narumi, A.; Yamada, M.; Unno, Y.; Kumaki, J.; Binder, W. H.; Enomoto, K.; Kikuchi, M.; Kawaguchi, S. *ACS Macro Letters* **2019**, *8* (6), 634–638. Copyright 2019 American Chemical Society. (C) AFM height image of a brush copolymer shows evidence of a branch point (white arrow). Reprinted with permission from Yu-Su, S. Y.; Sun, F. C.; Sheiko, S. S.; Konkolewicz, D.; Lee, H.-i.; Matyjaszewski, K. *Macromolecules* **2011**, *44* (15), 5928–5936. Copyright 2011 American Chemical Society. (D) AFM height map indicates asymmetric height profiles of cone-like bottlebrush polymers. The blue line in the plot shows a theoretical shape profile. Adapted with permission from Walsh, D. J.; Guironnet, D. *Proceedings of the National Academy of Sciences* **2019**, *116* (5), 1538–1542. (E) Graphene windows encapsulating polymer solutions to allow atomic-scale visualization of polystyrenesulfonate using LC-TEM. Adapted with permission from ref 69. Copyright 2017 Wiley-VCH Verlag GmbH & Co. KGaA.

dimensions of polymer chains. Flexible polymers in solution with globular conformations further obscure the possibility of imaging submolecular details.<sup>20</sup> Even for ultrahigh molecular weight polymers ( $M_w \approx 10^7$ ), diffraction-limited optical imaging hinders the ability to resolve distinct backbone conformations of synthetic polymer chains at equilibrium.<sup>45</sup> Super-resolution fluorescence microscopy<sup>48–50</sup> and scanning near-field optical microscopy<sup>51–53</sup> have garnered strong interest as methods to image polymers with 10 nm resolution, especially semiflexible polymers such as isocyanopeptides (Figure 4A).<sup>50</sup> However, the inherent dispersity in molecular weight distributions of synthetic polymers poses a formidable challenge to interpreting submolecular features.

Aside from fluorescence microscopy, atomic force microscopy (AFM) was the first<sup>6</sup> and most widely adopted<sup>54–58</sup> technique to image single synthetic polymers with sufficient contrast and spatial resolution. Tapping mode AFM allows for imaging in ambient conditions, wherein a cantilever is oscillated vertically near its resonant frequency while raster scanning the sample surface.<sup>59</sup> Cantilever–sample interactions are detected as phase or amplitude shifts to resolve nanometer-scale features without

contrast agents. Scanning across the surface allows millimeter-scale image generation to observe chain contours and populations of polymer molecules. AFM has resolved single biological, biohybrid, and synthetic polymers alike, from DNA<sup>60</sup> to isocyanopeptides<sup>61</sup> to polystyrene-*block*-poly(methyl methacrylate).<sup>62</sup> Tapping-mode AFM has proven particularly powerful for direct characterization of architecturally complex polymers, including ring polymers,<sup>39,63</sup> branched polymers,<sup>64</sup> and various bottlebrush polymers (Figure 4B–D).<sup>65–68</sup> Despite the widespread use of AFM for single polymer visualization, this method comes with several drawbacks: the temporal resolution of AFM is limited to the speed of the raster scan, and AFM remains a surface technique that complements quantitative bulk characterization.<sup>57</sup>

Liquid-cell transmission electron microscopy (LC-TEM) provides an alternative high-resolution approach that complements surface-based AFM imaging of single polymers. Recently, Granick and co-workers reported an exciting step forward in using LC-TEM to directly visualize single polymer dynamics at equilibrium in aqueous solution with subnanometer spatial resolution.<sup>69</sup> Here, polymer solutions were encapsulated in

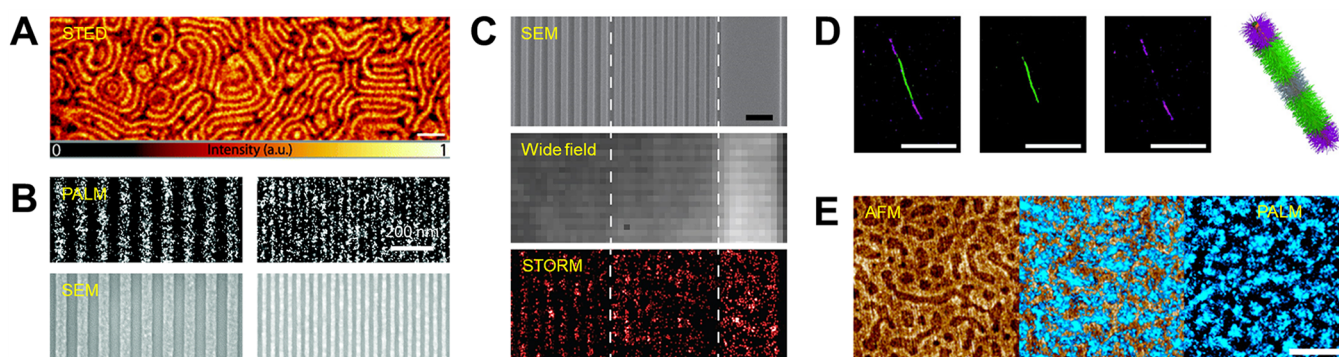


**Figure 5.** Polymer nanostructures visualized using super-resolution optical microscopy. (A) Stimulated emission depletion (STED) microscopy reveals the structure of poly(styrene-*block*-2-vinylpyridine) (PS-P2VP) swollen with PS homopolymer. The P2VP phase is selectively stained with ATTO-647N dye. Adapted with permission from Ullal, C. K.; Schmidt, R.; Hell, S. W.; Egner, A. *Nano Letters* **2009**, *9* (6), 2497–2500. Copyright 2009 American Chemical Society. (B) Photoactivatable localization microscopy (PALM) resolves nanopatterns etched into poly(methyl methacrylate) (PMMA) films. PMMA is doped with a rhodamine dye. Adapted with permission from ref 85. Copyright 2019 The Royal Society of Chemistry. (C) Label-free stochastic reconstruction optical microscopy (STORM) detects intrinsic fluorescent blinking events by PMMA to resolve nanopatterned features. Adapted with permission from ref 86. Copyright 2016 Nature Research. (D) Dye-containing block copolymers are assembled into cylindrical micelles, which are resolved using dual-color localization microscopy. Adapted with permission from ref 88. Copyright 2015 Wiley-VCH Verlag GmbH & Co. KGaA. (E) PS is copolymerized with vinyl-diarylethene for super-resolution imaging of assembled nanostructures in PS/PMMA blends. Adapted with permission from Qiang, Z.; Shebek, K. M.; Irie, M.; Wang, M. *ACS Macro Letters* **2018**, *7* (12), 1432–1437. Copyright 2018 American Chemical Society. Scale bars are (A) 500 nm, (B) 200 nm, (C) 500 nm, (D) 2  $\mu$ m, and (E) 1  $\mu$ m.

atomically thin graphene windows, which served dual purposes of sealing liquid samples that are typically incompatible with the high-vacuum TEM environment and enhancing contrast of polymer chains in the liquid.<sup>70</sup> Here, the dynamics of surface-adsorbed single polystyrenesulfonate and poly(ethylene oxide) chains were observed with subnanometer resolution and without heavy metal staining (Figure 4E), revealing sluggish surface diffusion behavior compared to single polymer diffusion in bulk solution. Slow chain diffusion was attributed to either segmental adsorption to graphene or the confined dimensions of the graphene windows.<sup>69</sup> Currently, LC-TEM imposes severe limits on the total imaging time, with radiolysis-induced bubble formation and polymer chain scission typically occurring within 100 s in water.<sup>69,71</sup> These effects can be mitigated by reducing the electron dose and modifying the solvent,<sup>71,72</sup> with such modifications resembling the use of photoprotective agents and limited radiation exposure during single-molecule fluorescence experiments.<sup>73,74</sup> Broadly speaking, further development of LC-TEM provides tremendous opportunities to answer fundamental questions in synthetic polymer chain dynamics and the solution-based assembly of polymers,<sup>75–77</sup> including “what are the roles of local flexibility and monomer aspect ratio on polymer dynamics?”<sup>18</sup> and “what are the mechanisms of nanostructure formation?”

## ■ PROBING SINGLE POLYMERS IN CONTEXT

Polymers rarely exist as single isolated chains. A major aim of single-polymer studies is to understand how molecular-scale behavior gives rise to bulk properties.<sup>78</sup> Despite recent progress, several challenges remain in leveraging the full power of single molecule techniques to study and understand polymer behavior in complicated chemical or physical environments. Polymer solutions,<sup>79</sup> gels,<sup>27–29,80–82</sup> melts,<sup>83</sup> and films<sup>51,52,84–88</sup> share crowded local chemical environments that impose nontrivial technical challenges to adapting fluorescence microscopy and AFM to investigate single chain behavior in these systems. To address these challenges, a broad array of single-molecule approaches can be used to study polymer materials, including tracking the motion of small-molecule probes,<sup>25–29,80–85</sup>

observing the conformations of tracer polymers in nondilute solutions or complex environments,<sup>79,87–89</sup> and extracting single untagged chains from solid-state environments.<sup>90–95</sup>

Fluorescent probe tracking has proven particularly effective for quantifying the formation and structure of polymer hydrogels, which are composed of water-swollen polymer networks. Fluorescent probe molecules diffuse freely in dilute polymer solutions; however, cross-linking of a polymer solution hinders the diffusion of probe molecules. Fluorescence correlation spectroscopy has been used to study probe diffusion in hydrogels, revealing a decrease in probe diffusivity as the degree of cross-linking increased.<sup>27</sup> This trend was also observed during the free-radical polymerization of a polymer gel, wherein fluorescent probes became trapped inside network pores and appeared immobile.<sup>28,29</sup> Recently, the network structures of pNIPAM-based microgels were quantified by combining 3D super-resolution microscopy with fluorophore-tagged cross-linking agents.<sup>80–82</sup> Integration of fluorophores into the polymer networks allowed for the direct observation of spatial heterogeneities across the bulk hydrogel mass. Reconstructed images of individual pNIPAM microgels revealed densely cross-linked centers surrounded by loosely cross-linked peripheral regions,<sup>80,82</sup> providing evidence for a nucleation-and-growth mechanism of microgel formation. These initial studies demonstrate the strong promise of super-resolution imaging and single-molecule approaches to revisit our understanding of polymer network formation, structure, and elasticity.

Super-resolution imaging has also gained traction as a nondestructive alternative to TEM for characterizing polymer nanostructures, including block copolymer assemblies<sup>84,87–89</sup> and nanopatterned polymers.<sup>85,86</sup> One approach to prepare polymer samples for fluorescence microscopy resembles that of TEM sample preparation. Here, polymer structures are either intrinsically fluorescent<sup>86</sup> or selectively stained with fluorescent dyes<sup>84,85</sup> and resolved using localization microscopy (Figure 5A–C). On the other hand, covalent attachment of fluorophores to the polymer chain (Figure 5D,E)<sup>87–89</sup> enables direct visualization of assembly and evolution of dynamic nanostructures.<sup>87</sup> Although single chain conformations have yet

to be resolved within polymer nanostructures, super-resolution microscopy provides promising avenues toward this goal.

The extraction of single chains from polymer crystals<sup>90–95</sup> and nanoparticles<sup>96</sup> has demonstrated the successful measurement of single polymer properties in the context of bulk and solid-state materials. Zhang and co-workers contributed both technological advances and structural insights toward crystalline polymers in their comprehensive series of AFM-based single-chain extraction experiments.<sup>90–95</sup> The development of solvent-free, air-phase SMFS improved force precision by reducing adhesion peaks that resulted from capillary bridging at the solvent–air interface.<sup>92</sup> This technique was compatible with both non-specific and specific tip–sample contact events, leading to single chain extraction. For nonspecific tip–sample contact, silicon or silanized AFM cantilevers underwent an approach–contact–retract movement at the surface of polymer single crystals, and approximately 1% of these movements produced successful force–extension curves.<sup>91,93,94</sup> For specific tip–sample contact, single crystals generated from thiol-terminated polymers were probed with gold-coated cantilevers, increasing the success rate to approximately 5% of approach events.<sup>90,92,95,96</sup> Importantly, terminal chain modifications are expected to have less influence on chain properties than fluorescent dyes along a polymer contour for imaging.

AFM-based SMFS investigations of polymer single crystals revealed molecular-scale information about the structure and thermal stability of crystalline polymers including polyamides,<sup>91,93</sup> polycaprolactone,<sup>93,94</sup> poly(ethylene oxide),<sup>90,92,95</sup> and poly-L-lactic acid.<sup>93,94</sup> Single-chain extraction curves quantified interactions between folded segments embedded in the polymer crystals, with specific motions corresponding to packing structures and unfolding mechanisms. Polyamide (PA) crystals with strong hydrogen bonding networks exhibited cooperative stick–slip motions, which manifest as hierarchical sawtooth-like force–extension curves (Figure 6A,B).<sup>91</sup> Larger peaks corresponded to the unfolding of segments in the crystal, and smaller peaks suggested “slipping” during hydrogen bond rearrangement. A comparison of smaller peaks between PA 6 and PA 66 revealed distinct slipping mechanisms: PA 66 consistently shifted by distances of approximately one hydrogen bonding repeat unit, whereas PA 6 shifted according to a bimodal distribution around the lengths of one or two repeat units. This bimodal distribution was attributed to alternating hydrogen-bonding atoms along the PA 66 backbone and suggested rotation of PA 66 chains upon extraction from the single crystal.<sup>91</sup> Stick–slip behavior was also shown to correspond directly to polymer chain conformation, such that zigzag-like chains (PA 6, PA 66, polycaprolactone) produce larger fluctuations that facilitate stick–slip motion, whereas helical chains (poly(ethylene oxide) and poly-L-lactic acid) undergo smooth chain extraction (Figure 6C).<sup>94</sup> Single chain extraction from poly(ethylene oxide) crystals generally required higher extraction forces from larger polymer crystals, suggesting a correlation between crystal domain size and mechanical stability.<sup>95</sup> The repetitive nature of crystalline polymers enabled direct molecular-scale investigations of highly relevant materials using AFM-based SMFS, and the expansion toward other materials with clever molecular designs is currently under way.<sup>96,97</sup>

## CONCLUSIONS AND OUTLOOK

Single-molecule techniques provide a direct window into viewing the formation, structure, and dynamics of synthetic

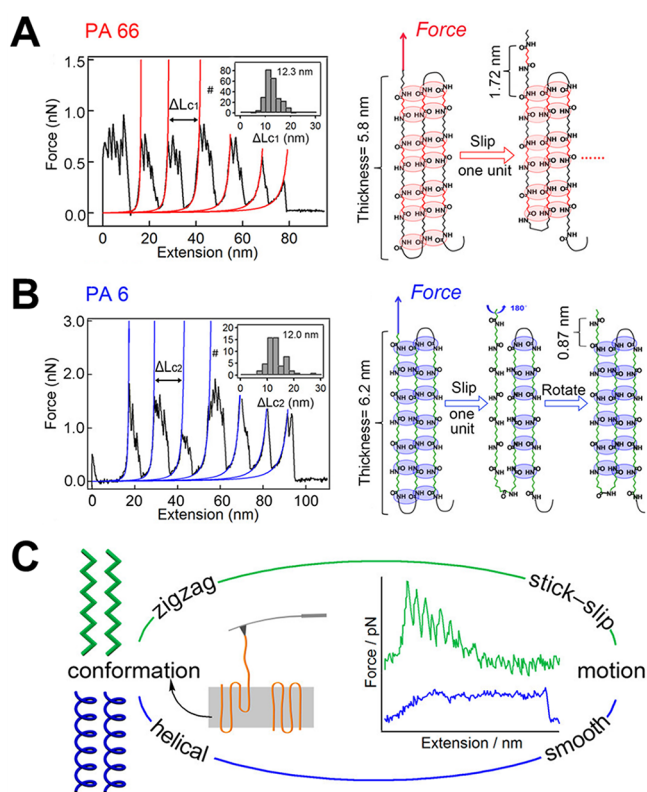


**Figure 6.** Force–extension curves suggest molecular-scale structure of crystalline polymers (A) PA 66 and (B) PA 6. Hierarchical sawtooth-like patterns reflect the unfolding of polyamide chains (large peaks), which includes slipping of single repeat units due to hydrogen bonding (small peaks). Contour length increments between major peaks ( $\Delta L_C$ ) are estimated using worm-like chain fits. Schematics show hydrogen bonding in PA 66 and PA 6 crystals gives rise to distinct slipping mechanisms. Adapted with permission from Lyu, X.; Song, Y.; Feng, W.; Zhang, W. *ACS Macro Letters* **2018**, *7* (6), 762–766. Copyright 2018 American Chemical Society. (C) Polymer crystals with helical chain packing do not exhibit jagged stick–slip force–extension curves observed from polymers with zigzag conformations. Reprinted with permission from Song, Y.; Ma, Z.; Yang, P.; Zhang, X.; Lyu, X.; Jiang, K.; Zhang, W. *Macromolecules* **2019**, *52* (3), 1327–1333. Copyright 2019 American Chemical Society.

polymer chains. In recent years, major advances in synthesis, imaging, and force spectroscopy have coalesced to enable broad exploration of polymers with diverse chemistries and structures. In this Viewpoint, we explore recent investigations of single monomer insertion kinetics, single chain visualization, and single polymers in the context of bulk materials.

Although most single-molecule techniques are inherently low in throughput, these methods provide for ultimate resolution of submolecular features and interrogation of heterogeneous molecular ensembles. In this way, single polymer studies provide necessary information that will enable bottom-up design of functional polymeric materials. As polymeric materials occupy an expanding functional landscape that includes charge transport,<sup>98</sup> selective mass transport,<sup>99</sup> self-healing behavior,<sup>100</sup> and controlled degradation,<sup>101</sup> we anticipate a similar expansion of single-polymer techniques to understand the role of polymer heterogeneity, sequence, and architecture in these applications. A key example includes the recent use of a scanning tunneling microscopy–break junction technique to understand the role of monomer sequence on molecular conductance in synthetic

oligomers.<sup>102</sup> This work revealed unexpected charge transport pathways in sequence-defined conjugated oligomers, such that specific monomer sequences exhibited order-of-magnitude enhancements in molecular conductance.

Importantly, single polymer experiments reach their full potential when complemented by classical characterization methods, thereby providing access to the complete spectrum of relevant time and length scales of polymeric materials. Looking forward, single polymer investigations will continue to provide answers to previously unsolved questions regarding the structure and dynamics of crystalline polymers, nanostructured polymers, polymer-laden interfaces, polymer networks, polymer glasses, and sequence-defined macromolecules.

## AUTHOR INFORMATION

### Corresponding Authors

**Danielle J. Mai** – Department of Chemical Engineering, Stanford University, Stanford, California 94305, United States; [orcid.org/0000-0001-5447-2845](https://orcid.org/0000-0001-5447-2845); Email: [djmai@stanford.edu](mailto:djmai@stanford.edu)

**Charles M. Schroeder** – Department of Materials Science and Engineering, Department of Chemical and Biomolecular Engineering, Beckman Institute for Advanced Science and Technology, University of Illinois at Urbana–Champaign, Urbana, Illinois 61801, United States; [orcid.org/0000-0001-6023-2274](https://orcid.org/0000-0001-6023-2274); Email: [cms@illinois.edu](mailto:cms@illinois.edu)

Complete contact information is available at:  
<https://pubs.acs.org/10.1021/acsmacrolett.0c00523>

### Notes

The authors declare no competing financial interest.

## ACKNOWLEDGMENTS

This work was supported by the Department of Chemical Engineering at Stanford University (DJM) and by the National Science Foundation through Grant CBET-1604038 (CMS).

## REFERENCES

- (1) Staudinger, H. Über Polymerisation. *Ber. Dtsch. Chem. Ges. B* **1920**, *53* (6), 1073–1085.
- (2) Müllhaupt, R. Hermann Staudinger and the Origin of Macromolecular Chemistry. *Angew. Chem., Int. Ed.* **2004**, *43* (9), 1054–1063.
- (3) Houseal, T. W.; Bustamante, C.; Stump, R. F.; Maestre, M. F. Real-time imaging of single DNA molecules with fluorescence microscopy. *Biophys. J.* **1989**, *56* (3), 507–516.
- (4) Smith, S.; Finzi, L.; Bustamante, C. Direct mechanical measurements of the elasticity of single DNA molecules by using magnetic beads. *Science* **1992**, *258* (5085), 1122–1126.
- (5) Perkins, T.; Smith, D.; Chu, S. Direct observation of tube-like motion of a single polymer chain. *Science* **1994**, *264* (5160), 819–822.
- (6) Marti, O.; Ribi, H.; Drake, B.; Albrecht, T.; Quate, C.; Hansma, P. Atomic force microscopy of an organic monolayer. *Science* **1988**, *239* (4835), 50–52.
- (7) Rief, M. Single Molecule Force Spectroscopy on Polysaccharides by Atomic Force Microscopy. *Science* **1997**, *275* (5304), 1295–1297.
- (8) Neuman, K. C.; Nagy, A. Single-molecule force spectroscopy: optical tweezers, magnetic tweezers and atomic force microscopy. *Nat. Methods* **2008**, *5* (6), 491–505.
- (9) de Gennes, P. G. Molecular Individualism. *Science* **1997**, *276* (5321), 1999.
- (10) Perkins, T. T. Single Polymer Dynamics in an Elongational Flow. *Science* **1997**, *276* (5321), 2016–2021.
- (11) Schroeder, C. M. Observation of Polymer Conformation Hysteresis in Extensional Flow. *Science* **2003**, *301* (5639), 1515–1519.
- (12) Mai, D. J.; Schroeder, C. M. Single polymer dynamics of topologically complex DNA. *Curr. Opin. Colloid Interface Sci.* **2016**, *26*, 28–40.
- (13) Hsiao, K.-W.; Sasmal, C.; Ravi Prakash, J.; Schroeder, C. M. Direct observation of DNA dynamics in semidilute solutions in extensional flow. *J. Rheol.* **2017**, *61* (1), 151–167.
- (14) Mai, D. J.; Saadat, A.; Khomami, B.; Schroeder, C. M. Stretching Dynamics of Single Comb Polymers in Extensional Flow. *Macromolecules* **2018**, *51* (4), 1507–1517.
- (15) Kikuchi, H.; Yokoyama, N.; Kajiyama, T. Direct Measurements of Stretching Force-Chain Ends Elongation Relationships of a Single Polystyrene Chain in Dilute Solution. *Chem. Lett.* **1997**, *26* (11), 1107–1108.
- (16) Jensenius, H.; Zocchi, G. Measuring the Spring Constant of a Single Polymer Chain. *Phys. Rev. Lett.* **1997**, *79* (25), 5030–5033.
- (17) de Gennes, P. G.; Gennes, P. P. G.; Press, C. U. *Scaling Concepts in Polymer Physics*; Cornell University Press, 1979.
- (18) Schroeder, C. M. Single polymer dynamics for molecular rheology. *J. Rheol.* **2018**, *62* (1), 371–403.
- (19) Pan, S.; Nguyen, D. A.; Sridhar, T.; Sunthar, P.; Prakash, J. R. Universal solvent quality crossover of the zero shear rate viscosity of semidilute DNA solutions. *J. Rheol.* **2014**, *58* (2), 339–368.
- (20) Latinwo, F.; Schroeder, C. M. Model systems for single molecule polymer dynamics. *Soft Matter* **2011**, *7* (18), 7907.
- (21) Smith, S. B.; Cui, Y.; Bustamante, C. Overstretching B-DNA: The Elastic Response of Individual Double-Stranded and Single-Stranded DNA Molecules. *Science* **1996**, *271* (5250), 795–799.
- (22) Janshoff, A.; Neitzert, M.; Oberdörfer, Y.; Fuchs, H. Force Spectroscopy of Molecular Systems—Single Molecule Spectroscopy of Polymers and Biomolecules. *Angew. Chem., Int. Ed.* **2000**, *39* (18), 3212–3237.
- (23) Giannotti, M. I.; Vancso, G. J. Interrogation of Single Synthetic Polymer Chains and Polysaccharides by AFM-Based Force Spectroscopy. *ChemPhysChem* **2007**, *8* (16), 2290–2307.
- (24) Lin, T.-S.; Coley, C. W.; Mochigase, H.; Beech, H. K.; Wang, W.; Wang, Z.; Woods, E.; Craig, S. L.; Johnson, J. A.; Kalow, J. A.; Jensen, K. F.; Olsen, B. D. BigSMILES: A Structurally-Based Line Notation for Describing Macromolecules. *ACS Cent. Sci.* **2019**, *5* (9), 1523–1531.
- (25) Nölle, J. M.; Primpke, S.; Müllen, K.; Vana, P.; Wöll, D. Diffusion of single molecular and macromolecular probes during the free radical bulk polymerization of MMA – towards a better understanding of the Trommsdorff effect on a molecular level. *Polym. Chem.* **2016**, *7* (24), 4100–4105.
- (26) Dorfschmid, M.; Müllen, K.; Zumbusch, A.; Wöll, D. Translational and Rotational Diffusion during Radical Bulk Polymerization: A Comparative Investigation by Full Correlation Fluorescence Correlation Spectroscopy (fcFCS). *Macromolecules* **2010**, *43* (14), 6174–6179.
- (27) Michelman-Ribeiro, A.; Boukari, H.; Nossal, R.; Horkay, F. Structural Changes in Polymer Gels Probed by Fluorescence Correlation Spectroscopy. *Macromolecules* **2004**, *37* (26), 10212–10214.
- (28) Wöll, D.; Uji-i, H.; Schnitzler, T.; Hotta, J.-i.; Dedecker, P.; Herrmann, A.; De Schryver, F. C.; Müllen, K.; Hofkens, J. Radical Polymerization Tracked by Single Molecule Spectroscopy. *Angew. Chem., Int. Ed.* **2008**, *47* (4), 783–787.
- (29) Stempfle, B.; Dill, M.; Winterhalter, M. J.; Müllen, K.; Wöll, D. Single molecule diffusion and its heterogeneity during the bulk radical polymerization of styrene and methyl methacrylate. *Polym. Chem.* **2012**, *3* (9), 2456–2463.
- (30) Tischer, T.; Gralla-Koser, R.; Trouillet, V.; Barner, L.; Barner-Kowollik, C.; Lee-Thedieck, C. Direct Mapping of RAFT Controlled Macromolecular Growth on Surfaces via Single Molecule Force Spectroscopy. *ACS Macro Lett.* **2016**, *5* (4), 498–503.
- (31) Liu, C.; Kubo, K.; Wang, E.; Han, K.-S.; Yang, F.; Chen, G.; Escobedo, F. A.; Coates, G. W.; Chen, P. Single polymer growth dynamics. *Science* **2017**, *358* (6361), 352–355.
- (32) Bouchiat, C.; Wang, M. D.; Allemand, J. F.; Strick, T.; Block, S. M.; Croquette, V. Estimating the Persistence Length of a Worm-Like

Chain Molecule from Force-Extension Measurements. *Biophys. J.* **1999**, *76* (1), 409–413.

(33) Easter, Q. T.; Blum, S. A. Single Turnover at Molecular Polymerization Catalysts Reveals Spatiotemporally Resolved Reactions. *Angew. Chem., Int. Ed.* **2017**, *56* (44), 13772–13775.

(34) Easter, Q. T.; Blum, S. A. Kinetics of the Same Reaction Monitored over Nine Orders of Magnitude in Concentration: When Are Unique Subensemble and Single-Turnover Reactivity Displayed? *Angew. Chem., Int. Ed.* **2018**, *57* (37), 12027–12032.

(35) Easter, Q. T.; Blum, S. A. Evidence for Dynamic Chemical Kinetics at Individual Molecular Ruthenium Catalysts. *Angew. Chem., Int. Ed.* **2018**, *57* (6), 1572–1575.

(36) Easter, Q. T.; Blum, S. A. Organic and Organometallic Chemistry at the Single-Molecule, -Particle, and -Molecular-Catalyst-Turnover Level by Fluorescence Microscopy. *Acc. Chem. Res.* **2019**, *52* (8), 2244–2255.

(37) Easter, Q. T.; Garcia, A.; Blum, S. A. Single-Polymer-Particle Growth Kinetics with Molecular Catalyst Speciation and Single-Turnover Imaging. *ACS Catal.* **2019**, *9* (4), 3375–3383.

(38) Yin, J.-F.; Hu, Y.; Wang, D.-G.; Yang, L.; Jin, Z.; Zhang, Y.; Kuang, G.-C. Cucurbit[8]uril-Based Water-Soluble Supramolecular Dendronized Polymer: Evidence from Single Polymer Chain Morphology and Force Spectroscopy. *ACS Macro Lett.* **2017**, *6* (2), 139–143.

(39) Narumi, A.; Yamada, M.; Unno, Y.; Kumaki, J.; Binder, W. H.; Enomoto, K.; Kikuchi, M.; Kawaguchi, S. Evaluation of Ring Expansion-Controlled Radical Polymerization System by AFM Observation. *ACS Macro Lett.* **2019**, *8* (6), 634–638.

(40) Pulcu, G. S.; Galenkamp, N. S.; Qing, Y.; Gasparini, G.; Mikhailova, E.; Matile, S.; Bayley, H. Single-Molecule Kinetics of Growth and Degradation of Cell-Penetrating Poly(disulfide)s. *J. Am. Chem. Soc.* **2019**, *141* (32), 12444–12447.

(41) Mai, D. J.; Brockman, C.; Schroeder, C. M. Microfluidic systems for single DNA dynamics. *Soft Matter* **2012**, *8* (41), 10560–10572.

(42) Shenoy, A.; Rao, C. V.; Schroeder, C. M. Stokes trap for multiplexed particle manipulation and assembly using fluidics. *Proc. Natl. Acad. Sci. U. S. A.* **2016**, *113*, 3976–3981.

(43) Kumar, D.; Shenoy, A.; Li, S.; Schroeder, C. M. Orientation control and nonlinear trajectory tracking of colloidal particles using microfluidics. *Physical Review Fluids* **2019**, *4* (11), 114203.

(44) Li, S.; Schroeder, C. M. Synthesis and Direct Observation of Thermoresponsive DNA Copolymers. *ACS Macro Lett.* **2018**, *7* (3), 281–286.

(45) Wang, Y.; Warshawsky, A.; Wang, C.; Kahana, N.; Chevillard, C.; Steinberg, V. Fluorescent ultrahigh-molecular-weight polyacrylamide probes for dynamic flow systems: Synthesis, conformational behavior and imaging. *Macromol. Chem. Phys.* **2002**, *203* (12), 1833–1843.

(46) Libera, M. R.; Egerton, R. F. Advances in the Transmission Electron Microscopy of Polymers. *Polym. Rev.* **2010**, *50* (3), 321–339.

(47) Kuei, B.; Aplan, M. P.; Litofsky, J. H.; Gomez, E. D. New opportunities in transmission electron microscopy of polymers. *Mater. Sci. Eng., R* **2020**, *139*, 100516.

(48) Muls, B.; Uji-i, H.; Melnikov, S.; Moussa, A.; Verheijen, W.; Soumillion, J.-P.; Josemon, J.; Müllen, K.; Hofkens, J. Direct Measurement of the End-to-End Distance of Individual Polyfluorene Polymer Chains. *ChemPhysChem* **2005**, *6* (11), 2286–2294.

(49) Aoki, H.; Mori, K.; Ito, S. Conformational analysis of single polymer chains in three dimensions by super-resolution fluorescence microscopy. *Soft Matter* **2012**, *8* (16), 4390–4395.

(50) Keshavarz, M.; Engelkamp, H.; Xu, J.; Braeken, E.; Otten, M. B. J.; Uji-i, H.; Schwartz, E.; Koepf, M.; Vananroye, A.; Vermant, J.; Nolte, R. J. M.; De Schryver, F.; Maan, J. C.; Hofkens, J.; Christianen, P. C. M.; Rowan, A. E. Nanoscale Study of Polymer Dynamics. *ACS Nano* **2016**, *10* (1), 1434–1441.

(51) Ube, T.; Aoki, H.; Ito, S.; Horinaka, J.-i.; Takigawa, T. Conformation of single PMMA chain in uniaxially stretched film studied by scanning near-field optical microscopy. *Polymer* **2007**, *48* (21), 6221–6225.

(52) Aoki, H.; Morita, S.; Sekine, R.; Ito, S. Conformation of Single Poly(methyl methacrylate) Chains in an Ultra-Thin Film Studied by Scanning Near-Field Optical Microscopy. *Polym. J.* **2008**, *40* (3), 274–280.

(53) Tamai, Y.; Sekine, R.; Aoki, H.; Ito, S. Conformation of Single Homopolymer Chain in Microphase-Separated Block Copolymer Monolayer Studied by Scanning Near-Field Optical Microscopy. *Macromolecules* **2009**, *42* (12), 4224–4229.

(54) Sheiko, S. S.; Möller, M. Visualization of Macromolecules A First Step to Manipulation and Controlled Response. *Chem. Rev.* **2001**, *101* (12), 4099–4124.

(55) Samori, P.; Surin, M.; Palermo, V.; Lazzaroni, R.; Leclère, P. Functional polymers: scanning force microscopy insights. *Phys. Chem. Chem. Phys.* **2006**, *8* (34), 3927–3938.

(56) Kumaki, J.; Sakurai, S.-i.; Yashima, E. Visualization of synthetic helical polymers by high-resolution atomic force microscopy. *Chem. Soc. Rev.* **2009**, *38* (3), 737–746.

(57) Sheiko, S. S.; Magonov, S. N. 2.23 - Scanning Probe Microscopy of Polymers. In *Polymer Science: A Comprehensive Reference*, Matyjaszewski, K., Möller, M., Eds.; Elsevier: Amsterdam, 2012; pp 559–605.

(58) Wang, D.; Russell, T. P. Advances in Atomic Force Microscopy for Probing Polymer Structure and Properties. *Macromolecules* **2018**, *51* (1), 3–24.

(59) Hölscher, H. AFM, Tapping Mode. In *Encyclopedia of Nanotechnology*; Bhushan, B., Ed.; Springer Netherlands: Dordrecht, 2012; pp 99–99.

(60) Hansma, H. G.; Vesenska, J.; Siegerist, C.; Kelderman, G.; Morret, H.; Sinsheimer, R. L.; Elings, V.; Bustamante, C.; Hansma, P. K. Reproducible Imaging and Dissection of Plasmid DNA Under Liquid with the Atomic Force Microscope. *Science* **1992**, *256* (5060), 1180–1184.

(61) Cornelissen, J. J. L. M.; Donners, J. J. J. M.; de Gelder, R.; Graswinckel, W. S.; Metselaar, G. A.; Rowan, A. E.; Sommerdijk, N. A. J. M.; Nolte, R. J. M.  $\beta$ -Helical Polymers from Isocyanopeptides. *Science* **2001**, *293* (5530), 676–680.

(62) Kumaki, J.; Nishikawa, Y.; Hashimoto, T. Visualization of Single-Chain Conformations of a Synthetic Polymer with Atomic Force Microscopy. *J. Am. Chem. Soc.* **1996**, *118* (13), 3321–3322.

(63) Xia, Y.; Boydston, A. J.; Grubbs, R. H. Synthesis and Direct Imaging of Ultrahigh Molecular Weight Cyclic Brush Polymers. *Angew. Chem., Int. Ed.* **2011**, *50* (26), 5882–5885.

(64) Yu-Su, S. Y.; Sun, F. C.; Sheiko, S. S.; Konkolewicz, D.; Lee, H.-i.; Matyjaszewski, K. Molecular Imaging and Analysis of Branching Topology in Polyacrylates by Atomic Force Microscopy. *Macromolecules* **2011**, *44* (15), 5928–5936.

(65) Daniel, W. F. M.; Burdyńska, J.; Vatankhah-Varnoosfaderani, M.; Matyjaszewski, K.; Paturej, J.; Rubinstein, M.; Dobrynin, A. V.; Sheiko, S. S. Solvent-free, supersonic and superelastic bottlebrush melts and networks. *Nat. Mater.* **2016**, *15* (2), 183–189.

(66) Radzinski, S. C.; Foster, J. C.; Scannelli, S. J.; Weaver, J. R.; Arrington, K. J.; Matson, J. B. Tapered Bottlebrush Polymers: Cone-Shaped Nanostructures by Sequential Addition of Macromonomers. *ACS Macro Lett.* **2017**, *6* (10), 1175–1179.

(67) Walsh, D. J.; Dutta, S.; Sing, C. E.; Guirounet, D. Engineering of Molecular Geometry in Bottlebrush Polymers. *Macromolecules* **2019**, *52* (13), 4847–4857.

(68) Walsh, D. J.; Guirounet, D. Macromolecules with programmable shape, size, and chemistry. *Proc. Natl. Acad. Sci. U. S. A.* **2019**, *116* (5), 1538–1542.

(69) Nagamanasa, K. H.; Wang, H.; Granick, S. Liquid-Cell Electron Microscopy of Adsorbed Polymers. *Adv. Mater.* **2017**, *29* (41), 1703555.

(70) Liao, H.-G.; Zheng, H. Liquid Cell Transmission Electron Microscopy. *Annu. Rev. Phys. Chem.* **2016**, *67* (1), 719–747.

(71) Wang, H.; Nagamanasa, K. H.; Kim, Y.-J.; Kwon, O.-H.; Granick, S. Longer-Lasting Electron-Based Microscopy of Single Molecules in Aqueous Medium. *ACS Nano* **2018**, *12* (8), 8572–8578.

- (72) Wang, H.; Li, B.; Kim, Y.-J.; Kwon, O.-H.; Granick, S. Intermediate states of molecular self-assembly from liquid-cell electron microscopy. *Proc. Natl. Acad. Sci. U. S. A.* **2020**, *117* (3), 1283–1292.
- (73) Campos, L. A.; Liu, J.; Wang, X.; Ramanathan, R.; English, D. S.; Muñoz, V. A photoprotection strategy for microsecond-resolution single-molecule fluorescence spectroscopy. *Nat. Methods* **2011**, *8* (2), 143–146.
- (74) Reilly, D. T.; Kim, S. H.; Katzenellenbogen, J. A.; Schroeder, C. M. Fluorescent Nanoconjugate Derivatives with Enhanced Photostability for Single Molecule Imaging. *Anal. Chem.* **2015**, *87* (21), 11048–11057.
- (75) Li, C.; Tho, C. C.; Galaktionova, D.; Chen, X.; Král, P.; Mirsaidov, U. Dynamics of amphiphilic block copolymers in an aqueous solution: direct imaging of micelle formation and nanoparticle encapsulation. *Nanoscale* **2019**, *11* (5), 2299–2305.
- (76) Wu, H.; Friedrich, H.; Patterson, J. P.; Sommerdijk, N. A. J. M.; Jonge, N. Liquid-Phase Electron Microscopy for Soft Matter Science and Biology. *Adv. Mater.* **2020**, *32*, 2001582.
- (77) Early, J. T.; Yager, K. G.; Lodge, T. P. Direct Observation of Micelle Fragmentation via In Situ Liquid-Phase Transmission Electron Microscopy. *ACS Macro Lett.* **2020**, *9* (5), 756–761.
- (78) Chung, J.; Kushner, A. M.; Weisman, A. C.; Guan, Z. Direct correlation of single-molecule properties with bulk mechanical performance for the biomimetic design of polymers. *Nat. Mater.* **2014**, *13* (11), 1055–1062.
- (79) King, J. T.; Yu, C.; Wilson, W. L.; Granick, S. Super-Resolution Study of Polymer Mobility Fluctuations near  $c^*$ . *ACS Nano* **2014**, *8* (9), 8802–8809.
- (80) Karanastasis, A. A.; Zhang, Y.; Kenath, G. S.; Lessard, M. D.; Bewersdorf, J.; Ullal, C. K. 3D mapping of nanoscale crosslink heterogeneities in microgels. *Mater. Horiz.* **2018**, *5* (6), 1130–1136.
- (81) Karanastasis, A. A.; Kenath, G. S.; Sundararaman, R.; Ullal, C. K. Quantification of functional crosslinker reaction kinetics via super-resolution microscopy of swollen microgels. *Soft Matter* **2019**, *15* (45), 9336–9342.
- (82) Siemes, E.; Nevskiy, O.; Sysoiev, D.; Turnhoff, S. K.; Oppermann, A.; Huhn, T.; Richtering, W.; Wöll, D. Nanoscopic Visualization of Cross-Linking Density in Polymer Networks with Diarylethene Photoswitches. *Angew. Chem., Int. Ed.* **2018**, *57* (38), 12280–12284.
- (83) Krause, S.; Neumann, M.; Fröbe, M.; Magerle, R.; von Borczyskowski, C. Monitoring Nanoscale Deformations in a Drawn Polymer Melt with Single-Molecule Fluorescence Polarization Microscopy. *ACS Nano* **2016**, *10* (2), 1908–1917.
- (84) Ullal, C. K.; Schmidt, R.; Hell, S. W.; Egner, A. Block Copolymer Nanostructures Mapped by Far-Field Optics. *Nano Lett.* **2009**, *9* (6), 2497–2500.
- (85) Wang, M.; Marr, J. M.; Davanco, M.; Gilman, J. W.; Liddle, J. A. Nanoscale deformation in polymers revealed by single-molecule super-resolution localization–orientation microscopy. *Mater. Horiz.* **2019**, *6* (4), 817–825.
- (86) Urban, B. E.; Dong, B.; Nguyen, T.-Q.; Backman, V.; Sun, C.; Zhang, H. F. Subsurface Super-resolution Imaging of Unstained Polymer Nanostructures. *Sci. Rep.* **2016**, *6* (1), 28156.
- (87) Qiang, Z.; Shebek, K. M.; Irie, M.; Wang, M. A Polymerizable Photoswitchable Fluorophore for Super-Resolution Imaging of Polymer Self-Assembly and Dynamics. *ACS Macro Lett.* **2018**, *7* (12), 1432–1437.
- (88) Ullal, C. K.; Primpke, S.; Schmidt, R.; Böhm, U.; Egner, A.; Vana, P.; Hell, S. W. Flexible Microdomain Specific Staining of Block Copolymers for 3D Optical Nanoscopy. *Macromolecules* **2011**, *44* (19), 7508–7510.
- (89) Boott, C. E.; Laine, R. F.; Mahou, P.; Finnegan, J. R.; Leitao, E. M.; Webb, S. E. D.; Kaminski, C. F.; Manners, I. In Situ Visualization of Block Copolymer Self-Assembly in Organic Media by Super-Resolution Fluorescence Microscopy. *Chem. - Eur. J.* **2015**, *21* (51), 18539–18542.
- (90) Liu, K.; Song, Y.; Feng, W.; Liu, N.; Zhang, W.; Zhang, X. Extracting a Single Polyethylene Oxide Chain from a Single Crystal by a Combination of Atomic Force Microscopy Imaging and Single-Molecule Force Spectroscopy: Toward the Investigation of Molecular Interactions in Their Condensed States. *J. Am. Chem. Soc.* **2011**, *133* (10), 3226–3229.
- (91) Lyu, X.; Song, Y.; Feng, W.; Zhang, W. Direct Observation of Single-Molecule Stick–Slip Motion in Polyamide Single Crystals. *ACS Macro Lett.* **2018**, *7* (6), 762–766.
- (92) Yang, P.; Song, Y.; Feng, W.; Zhang, W. Unfolding of a Single Polymer Chain from the Single Crystal by Air-Phase Single-Molecule Force Spectroscopy: Toward Better Force Precision and More Accurate Description of Molecular Behaviors. *Macromolecules* **2018**, *51* (18), 7052–7060.
- (93) Ma, Z.; Yang, P.; Zhang, X.; Jiang, K.; Song, Y.; Zhang, W. Quantifying the Chain Folding in Polymer Single Crystals by Single-Molecule Force Spectroscopy. *ACS Macro Lett.* **2019**, *8* (9), 1194–1199.
- (94) Song, Y.; Ma, Z.; Yang, P.; Zhang, X.; Lyu, X.; Jiang, K.; Zhang, W. Single-Molecule Force Spectroscopy Study on Force-Induced Melting in Polymer Single Crystals: The Chain Conformation Matters. *Macromolecules* **2019**, *52* (3), 1327–1333.
- (95) Song, Y.; Yang, P.; Jiang, K.; Zhang, W. Force-induced melting of a single polyethylene oxide chain from single crystal: Molecular behavior and influencing factors. *Polymer Crystallization* **2019**, *2* (2), e10048.
- (96) Hosono, N.; Kushner, A. M.; Chung, J.; Palmans, A. R. A.; Guan, Z.; Meijer, E. W. Forced Unfolding of Single-Chain Polymeric Nanoparticles. *J. Am. Chem. Soc.* **2015**, *137* (21), 6880–6888.
- (97) Levy, A.; Feinstein, R.; Diesendruck, C. E. Mechanical Unfolding and Thermal Refolding of Single-Chain Nanoparticles Using Ligand–Metal Bonds. *J. Am. Chem. Soc.* **2019**, *141* (18), 7256–7260.
- (98) Gomez, E. D.; Panday, A.; Feng, E. H.; Chen, V.; Stone, G. M.; Minor, A. M.; Kisielowski, C.; Downing, K. H.; Borodin, O.; Smith, G. D.; Balsara, N. P. Effect of Ion Distribution on Conductivity of Block Copolymer Electrolytes. *Nano Lett.* **2009**, *9* (3), 1212–1216.
- (99) Yang, Y. J.; Mai, D. J.; Dursch, T. J.; Olsen, B. D. Nucleopore-Inspired Polymer Hydrogels for Selective Biomolecular Transport. *Biomacromolecules* **2018**, *19* (10), 3905–3916.
- (100) Tran, H.; Feig, V. R.; Liu, K.; Zheng, Y.; Bao, Z. Polymer Chemistries Underpinning Materials for Skin-Inspired Electronics. *Macromolecules* **2019**, *52* (11), 3965–3974.
- (101) Hernandez, H. L.; Kang, S.-K.; Lee, O. P.; Hwang, S.-W.; Kaitz, J. A.; Inci, B.; Park, C. W.; Chung, S.; Sottos, N. R.; Moore, J. S.; Rogers, J. A.; White, S. R. Triggered Transience of Metastable Poly-(phthalaldehyde) for Transient Electronics. *Adv. Mater.* **2014**, *26* (45), 7637–7642.
- (102) Yu, H.; Li, S.; Schwieter, K. E.; Liu, Y.; Sun, B.; Moore, J. S.; Schroeder, C. M. Charge Transport in Sequence-Defined Conjugated Oligomers. *J. Am. Chem. Soc.* **2020**, *142* (10), 4852–4861.